Journal of Maps

ISSN: (Print) (Online) Journal homepage: https://www.tandfonline.com/loi/tjom20

Salt sheet extrusion and emplacement within the South-Central Pyrenean fold-and-thrust belt: the Les Avellanes Diapir case-of-study

Gabriel Cofrade, Òscar Gratacós, Irene Cantarero, Oriol Ferrer, Pedro Ramirez-Perez, Eduard Roca & Anna Travé

To cite this article: Gabriel Cofrade, Òscar Gratacós, Irene Cantarero, Oriol Ferrer, Pedro Ramirez-Perez, Eduard Roca & Anna Travé (2023) Salt sheet extrusion and emplacement within the South-Central Pyrenean fold-and-thrust belt: the Les Avellanes Diapir case-of-study, Journal of Maps, 19:1, 2273834, DOI: 10.1080/17445647.2023.2273834

To link to this article: https://doi.org/10.1080/17445647.2023.2273834

JOURNAL OF MAPS
2023, VOL. 19, NO. 1, 2273834
https://doi.org/10.1080/17445647.2023.2273834

SCIENCE

OPEN ACCESS Check for updates

Salt sheet extrusion and emplacement within the South-Central Pyrenean fold-and-thrust belt: the Les Avellanes Diapir case-of-study

Gabriel Cofrade[a], Òscar Gratacós[b], Irene Cantarero[a], Oriol Ferrer[b], Pedro Ramirez-Perez[a], Eduard Roca[b] and Anna Travé[a]

[a]Institut de Recerca UB-Geomodels, Grup de recerca Geologia Sedimentaria, Departament de Mineralogia, Petrologia i Geologia Aplicada, Facultat de Ciències de la Terra, Universitat de Barcelona (UB), Barcelona, Spain; [b]Institut de Recerca UB-Geomodels, Grup de Geodinàmica i Anàlisi de Conques, Departament de Dinàmica de la Terra i de l'Oceà, Facultat de Ciències de la Terra, Universitat de Barcelona (UB), Barcelona, Spain.

ABSTRACT

A detailed geological map of the Les Avellanes salt Diapir (South-Central Pyrenees, Spain) that includes both the diapir body and adjacent areas is presented to understand the diapir evolution and geometry. Structural, stratigraphical, and sedimentary data north and south of the diapir is used to infer the timing of its emplacement. The northern diapir boundary is characterized by a set of extensional faults oblique to the main Pyrenean trend, while the southern boundary is an extrusive salt sheet that overlays the late Eocene-early Oligocene sequence in three adjacent sub-basins. Salt extrusion occurred due to synorogenic folding. The topography created as salt extruded trapped the arrival of external sediments from the north, blocking the transport pathways southward. Low sedimentation rates southwards allowed for the lateral salt extrusion, advancing southwards from the feeder. The salt sheet emplacement was postdated by Oligocene conglomerates, indicating that the salt extrusion was a relatively quick event.

ARTICLE HISTORY
Received 25 May 2023
Revised 18 September 2023
Accepted 16 October 2023

KEYWORDS
Diapir; salt sheet; Pyrenees; fold and thrust belt; tectonostratigraphy

1. Introduction

The study of salt diapirism in the South-Central Pyrenees has primarily focused on the internal regions of the South Pyrenean fold-and-thrust belt. During the Lower Cretaceous rifting stage, pre-orogenic diapirs developed in those regions (e.g. Cotiella Basin, Lopez-Mir et al., 2015; 2016, Sopeira Basin and Sant Gervàs Basin, Saura et al., 2016 and Organyà Basin, Casini et al., 2023) which were subsequently inverted during the Upper Cretaceous-Oligocene contraction (Beaumont et al., 2000; García-Senz, 2002; Martinez-Peña & Casas-Sainz, 2003; Ramos et al., 2020). However, the South Pyrenean external areas also contain several diapirs associated with syn-orogenic sedimentation and the southwards propagation of the Pyrenean deformation (Burrel & Teixell, 2021; Cofrade et al., 2023; Salvany, 1999; Santolaria et al., 2014; Santolaria et al., 2022b). These diapirs offer quality exposures for a direct field approach and provide insights into the relationship between tectonosedimentary processes and diapirism, thus shedding light on how salt interacts with mountain building processes (Duffy et al., 2018; Rowan et al., 2019; Santolaria et al., 2022a). Among these diapirs, the Les Avellanes Diapir, located next to the frontal Pyrenean thrust within the external South-Central Pyrenean region, shows one of the most extensive exposures and is an excellent field example that illustrates salt-sediment interaction during tectonic compression.

One approach to unravel the combination of tectonics, sedimentation, and diapirism is to map the diapir body as well as the adjacent areas using structural and sedimentary data (e.g. Sivas Basin, Turkey, Callot et al., 2016; Tazoult Salt Wall, Morocco, Martín-Martín et al., 2017; Flinders Range, Australia, Rowan et al., 2019; Vidal-Royo et al., 2021) as used in this work in the Southern Pyrenees. Geological maps from the Institut Cartogràfic i Geològic de Catalunya (ICGC, https://www.icgc.cat) in the eastern South Pyrenean area (1:25000 scale) (ICGC Figuerola de Meià sheet, 2007; ICGC Àger sheet, 2008; ICGC Os de Balaguer sheet, 2010 and ICGC Camarasa sheet, 2014), and the Mapa Geológico de España (1:50000 scale) (Os de Balaguer sheet by Teixell & Barnolas, 1996; Artesa de Segre sheet by Saula et al., 2000), as well as maps published in other geological reports (i.e. Burrel & Teixell, 2021; Lopez-Mir et al., 2016; Muñoz et al., 2018), have created an extensive cartographic

CONTACT Gabriel Cofrade gcofrade@ub.edu Institut de Recerca UB-Geomodels, Grup de recerca Geologia Sedimentaria, Departament de Mineralogia, Petrologia i Geologia Aplicada, Facultat de Ciències de la Terra, Universitat de Barcelona (UB), c/ Martí i Franquès s/n. 08028 Barcelona, Spain
Supplemental map for this article can be accessed at https://doi.org/10.1080/17445647.2023.2273834

database. However, geological mapping must be appropriate to the scale of the features portrayed to illustrate the range of geometries and structures produced during their geological evolution (Borradaile, 2015). Since diapirs are structures that can exhibit severe structural and stratigraphic changes in their surroundings regions (Roca et al., 2021; Rowan et al., 2019), it is necessary to improve current maps to reach the optimal scale required to observe salt-sediment interactions accurately.

In this regard, the Les Avellanes Diapir is located in a region of intense deformation where the pre-orogenic and syn-orogenic host sequence outcrops along compressive structures, constraining the diapir's evolution. At the SW boundary of the Les Avellanes Diapir, the salt body covers the syn-orogenic late Eocene-early Oligocene sequence which records the extrusion of the salt as an extrusive (subaerial) advancing salt sheet (Cofrade et al., 2023). This contribution presents a detailed geological map of the Les Avellanes Diapir (1:32000) that showcases the complete extension of the allochthonous salt-bedrock contact and the internal architecture of this diapir. The map combines structural, sedimentological, and stratigraphic observations to deduce the diapir geometry and evolution.

2. Geological context

The Pyrenees (Figure 1A) is an asymmetric, doubly-vergent orogenic belt formed by the continental collision between Iberia and Eurasia plates, from Late Cretaceous to Middle Miocene times (i.e. Beaumont et al., 2000; Calvet et al., 2021; Garcés et al., 2020; Muñoz, 1992; 2002; Muñoz et al., 2018; Sussman et al., 2004; Teixell & Muñoz, 2000; Vergés et al., 1995). The collision was caused by the eastward translation and counterclockwise drifting of the Iberian plate relative to Eurasia during the opening of the North Atlantic Ocean (Angrand & Mouthereau, 2021; Handy et al., 2010; Olivet, 1996; Sibuet et al., 2004). This deformation inverted the pre-existing Lower Cretaceous hyperextended margin, resulting in the formation of an antiformal sedimentológicos de las evaporitas del Triásico y del Liásico inferior en el E de la Península Ibérica. Cuadernos de Geología Ibérica stack of basement-detached, southward-imbricated thrust sheets known as the Axial Zone (Figure 1A) (Beaumont et al., 2000; Espurt et al., 2019; Martinez-Peña & Casas-Sainz, 2003; Muñoz, 1992; Odlum et al., 2019). The Axial Zone acts as a boundary between the North and South Pyrenean fold-and-thrust belts. The South Pyrenean fold-and-thrust belt, where the Les Avellanes Diapir is located, was formed by the southward propagation of the thrust front from the Axial Zone as an imbricated south-verging sequence of piggyback thrusts, detached along the Triassic evaporites (Figure 1B) (Muñoz, 1992; Muñoz et al., 2018; Saura et al., 2016; Séguret, 1972; Vergés et al., 2002; Vergés & Muñoz, 1990).

Specifically, the South-Central Pyrenean fold-and-thrust belt is formed of three main thrust sheets branching southwards from a sole thrust running along the Upper Triassic detachment and emplaced over the Eocene-Oligocene evaporites of the Ebro Foreland Basin (Figure 1C) (Muñoz, 1992; Vergés et al., 1995). These are, from north to south, the Bóixols-Cotiella Thrust Sheet, the Montsec-Peña Montañesa Thrust Sheet, and the Serres Marginals Thrust Sheet, emplaced during the late Cretaceous, the Paleogene-Eocene, and the late Eocene-Oligocene, respectively (Beaumont et al., 2000; Cruset et al., 2020; Garcés et al., 2020; Muñoz et al., 2013; Muñoz-López et al., 2022; Teixell & Muñoz, 2000). These three thrust sheets form an orogenic salient flanked by highly oblique tectonic structures (N-S to E-W) (Figure 1B). Differential tectonic transport displacement along-strike caused the gradual formation of the orogenic curvature (Garcés et al., 2020; Muñoz et al., 2013; Sussman et al., 2004). The larger tectonic transport of these thrust sheets was caused by the superposition of the two predominant décollement levels in the Pyrenees: the Upper-Middle Triassic evaporites and the upper Eocene-Oligocene evaporites in the Ebro Foreland Basin (Muñoz et al., 2013; 2018; Santolaria et al., 2022b)

The Les Avellanes salt Diapir is located at the frontal part of the thrust salient in the Serres Marginals Thrust Sheet. Here, the distribution and mobilization of the Triassic evaporites strongly controlled the mountain-building process, impacting the location, type, and geometry of contractional structures. In the Serres Marginals, Triassic exposures are associated with thrusts, detached folds (Salvany, 1999), and salt diapirs (García-Senz, 2002; McClay et al., 2004; Santolaria et al., 2014). Triassic outcrops are mainly formed of gypsum, carbonates, and mudrocks and salt is not exposed at the surface (Calvet et al., 2004; López-Gómez et al., 2019; Salvany & Bastida, 2004). However, exploration wells and gravimetric maps reveal the presence of subsurface Middle to Upper Triassic salt (Lanaja, 1987, e.g. Monzón-1 well log; Santolaria et al., 2014; Camara & Flinch, 2017; Ayala et al., 2021). These Triassic sequence was sedimented an epicontinental, restrictive marine-coastal evaporitic environment within a polyphase rifting that spans from the late Permian to Middle-Late Triassic associated with the fragmentation of the supercontinent Pangea and the opening of the North Atlantic Ocean (Ortí et al., 2017). In this sequence, there are two main salt intervals, middle Triassic (Ladinian, middle Muschelkalk facies, M2) and upper Triassic (Carnian to Norian, lower and middle Keuper facies, K1 and K2) in age respectively (Figure 2) (Calvet et al., 2004;

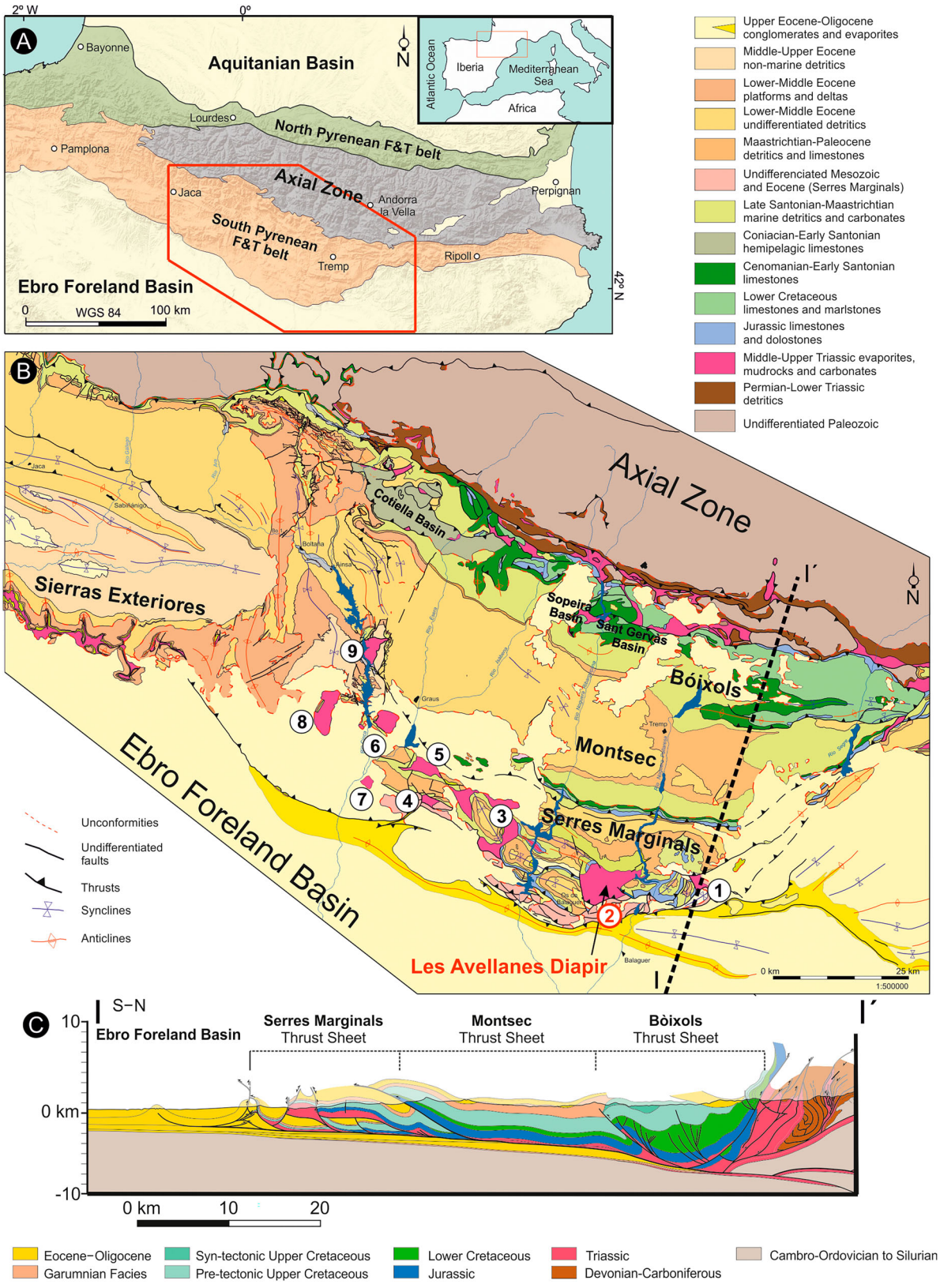

Figure 1. (A) Geological sketch of the Pyrenees. The red polygon indicates the approximate extension of Figure 1B. Modified from González-Esvertit et al., 2022. (B) Geological map of the South-Central Pyrenean fold-and-thrust belt. Modified from Muñoz et al., 2018. External diapirs are numbered: 1. Alòs de Balaguer, 2. Les Avellanes, 3. Estopinyà, 4. Calasanz, 5. Justeu, 6. La Puebla de Castro, 7. Estada, 8. Naval, and 9. Clamosa. (C) Section showing the structure of the South-Central Pyrenean fold-and-thrust belt. Black dashed line in Figure 1B indicates the location of this cross-section (after Muñoz et al., 2018).

Camara & Flinch, 2017; Klimowitz & Torrescusa, 1990; Ortí, 1987; Ortí et al., 1996). These salt intervals also contain interbedded sulphates and mudrocks, which are more abundant in the upper part of the Triassic sequence, in the K1-K2 salt interval (Jurado, 1990; Ortí et al., 1996). These two salt intervals are

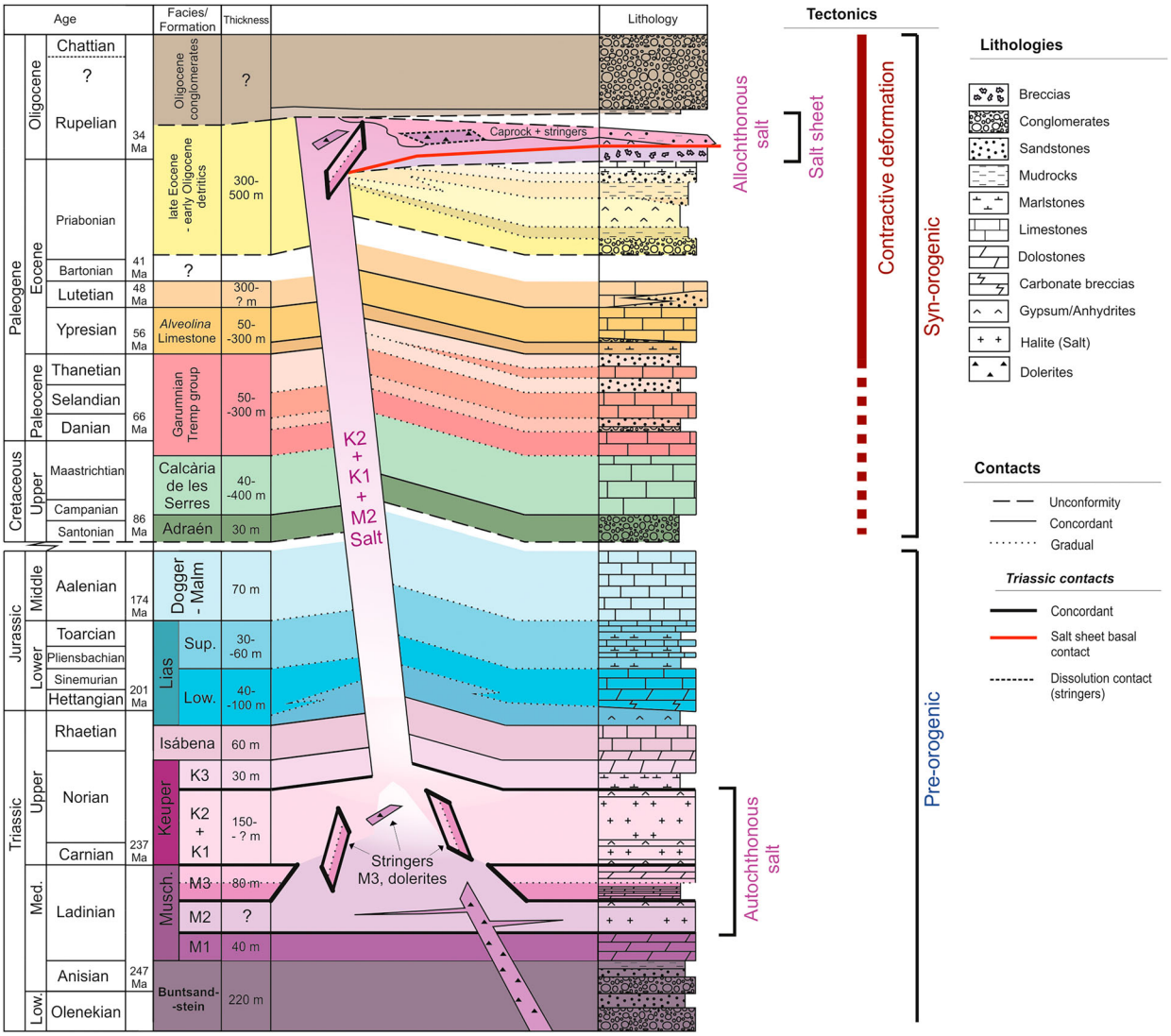

Figure 2. Sketch representing the stratigraphy of the Les Avellanes Diapir and adjacent areas, not-to-scale. Geometries are over-simplified to understand stratigraphic relationships. The thicknesses of the units are approximations (see sources from Cofrade et al., 2023).

separated by a late Ladinian carbonate layer that corresponds to the upper Muschelkalk facies (M3). Dolerites are also found within the salt sequence, intruding into the Muschelkalk and Keuper intervals as sills and/or dykes during or slightly after salt deposition (López-Gómez et al., 2019). During diapirism, the mobilization of the Triassic salt caused the detachment and rupture of the intrasalt Muschelkalk (M3) layer. Resulting fragments of the intrasalt carbonate strata, called stringers, behaved as competent bodies in the host salt (Cofrade et al., 2023). These stringers experienced intense deformation while being transported within the salt flow and accumulated at the surface due to salt dissolution. Thus, major Triassic exposures in the area, including the Les Avellanes Diapir body, are interpreted as caprock-like deposits formed by a caprock matrix constituted by dissolution residues (gypsum and mudrocks), that embeds decameter-thick and laterally extensive carbonate stringers and dolerite bodies (Cofrade et al., 2023). Dolerite bodies were also probably transported within the salt flow and accumulated at the surface as salt dissolved.

The Les Avellanes Diapir is surrounded by a southward wedging sedimentary host sequence. This sequence is formed from the erosion and condensed deposition occurring at the southernmost tip of the Pyrenean basin (former location of the Serres Marginals Thrusts Sheet), detached along the Triassic salt and tectonically emplaced over the Ebro Foreland Basin (Garcés et al., 2020; Muñoz et al., 2018). This host sequence spans from the Upper Triassic to the Oligocene and can be subdivided into a pre-orogenic and a syn-orogenic interval (Figure 2).

The pre-orogenic sequence is constituted of an alternation of white marls and dolostones (Norian in age), which is the top of the Keuper facies, K3; followed by well-bedded dolostones and limestones of the Isábena/Imón Fm. (Rhaetian in age). These units are overlain by a marine Jurassic succession (Pocoví, 1978) formed of lower Lias evaporites and breccias,

upper Lias marls with interbedded limestones, and Dogger-Malm platform carbonates.

The syn-orogenic sequence in the studied area began with the sedimentation of the Upper Cretaceous sediments, consisting of a basal unit of sandstones and conglomerates from the Adraén Fm. (Santonian in age), which unconformably overlays the Jurassic rocks (Figure 2) (Pocoví, 1978; Ullastre & Masriera, 2004). The marine limestones and calcareous sandstones from the Calcària de les Serres Fm. (Maastrichtian in age) overlie the Adraén Fm. The Upper Cretaceous gradually evolves into a continental siliciclastic-calcareous alternation named the Tremp Group (also known as Garumnian facies), which represents a marine regression that occurred during the Cretaceous-Paleocene boundary (Gómez-Gras et al., 2016). This episode was followed by a new transgression during the early Eocene (early Ypresian times) (Pujalte et al., 2009), represented by the marine *Alveolina* Limestones characterized by their content of *Alveolina* (Pocoví, 1978). The basal horizon of this unit is easily recognizable in the field, being useful for regional correlations. South of the diapir, the *Alveolina* Limestones gradually change into more siliciclastic, shallower facies during the Lutetian, which are almost missing elsewhere in the Serres Marginals. After that, late Eocene-early Oligocene mixed clastic and evaporitic facies covered the structural paleorelief produced by the uplift and ongoing formation of tectonic structures in the Serres Marginals, therefore recording the orogenic deformation at the external Pyrenean wedge (Teixell & Muñoz, 2000) and at the foreland basin (Ramirez-Perez et al., 2023; Santolaria et al., 2022b). Oligocene deposition postdating the contractional structures, buried the fold-and-thrust belt under more than 700 m of conglomerates in the Les Avellanes Diapir area (Fillon et al., 2013). Finally, the Pleistocene erosion sculpted the present relief.

3. Methods

The geological map of the Les Avellanes Diapir covers an area of approximately 200 km^2. It is presented at a scale of 1:32000 (Main Map, Figure 3) but the cartography work was done at a detailed scale of 1:10.000. The map was created through several months of fieldwork and is also based on the existing geological maps (ICGC Figuerola de Meià sheet, 2007; ICGC Àger sheet, 2008; ICGC Os de Balaguer sheet, 2010 and ICGC Camarasa sheet, 2014, and Os de Balaguer sheet by Teixell & Barnolas, 1996; Artesa de Segre sheet by Saula et al., 2000). The topographic base comprised of the 1:25000 and 1:5000 maps and orthophotographic aerial images (25 cm pixel maximum resolution) from the ICGC (series 25 cm (OF-25C) v4r0, 2022 flight), as well as a high-resolution DEM (ICGC, HD-DEM, 2 × 2 m (MET-2) v2.0 (2016–2017), https://icgc.cat). Structural data (up to 3000 dip directions/dip angles from bedding surfaces, faults, and foliations) was collected directly on the field with a compass-clinometer, georeferenced with FieldMove software, and digitalized alongside surfaces and stratigraphic contacts with ArcGIS software. Fault symbology is simplified based on stratigraphic constraints to avoid the complexity caused by the inversion, tilting, and/or reactivations during the intense deformation history of the area. The map is accompanied by a stratigraphic key, which is divided into pre- and syn-orogenic lithostratigraphic units and the diapir units, as well as a stratigraphical sketch summarizing the relationships between these units in the area. Quaternary deposits have not been included on the map.

4. Results

4.1. Structural domains of the Les Avellanes Diapir adjacent areas

The Les Avellanes Diapir has an irregular shape produced by the combination of tectonic structures and diapirism, resulting in different structural domains. These are described below regarding their location relative to the diapir boundaries (Main Map and Figure 3).

Along the northern boundary of the diapir, the contact between the diapir body and the host sedimentary sequence runs along the trace of two sets of faults, NW-SE and SW-NE, oblique to the main compressional structures in this area (W-E). The north-central part of the Les Avellanes Diapir exposure is located in the intersection of both sets of faults. Towards the NE and NW areas, these faults extend outwards and cut through the folded Jurassic to Eocene sequence, resulting in grabens (Main Map, Figure 3). Accordingly, these faults are evaluated as extensional, regardless of the relationship observed along the diapir contact, which resulted from the diapir emplacement. They were formed during the Eocene-Oligocene since Oligocene conglomerates filled the grabens and postdate the faults at the NE and NW areas.

Adjacent to the western boundary of the Les Avellanes Diapir, the structure is characterized by a set of NW-SE trending folds affecting the salt-detached Jurassic to Oligocene Serres Marginals sequence. The fold wavelength gradually decreases southwards as the detached sequence becomes thinner. Broad synclines are tectonically imbricated, separated by thrusts and back-thrusts with the Keuper facies outcropping along the base of the hangingwall (e.g. along the Os de Balaguer back-thrust, Figure 3 and Main Map). In addition, the Ypresian *Alveolina* Limestones exhibit rotational offlap to onlap growth strata architectures close to the fold limbs (Cofrade et al., 2023), indicating

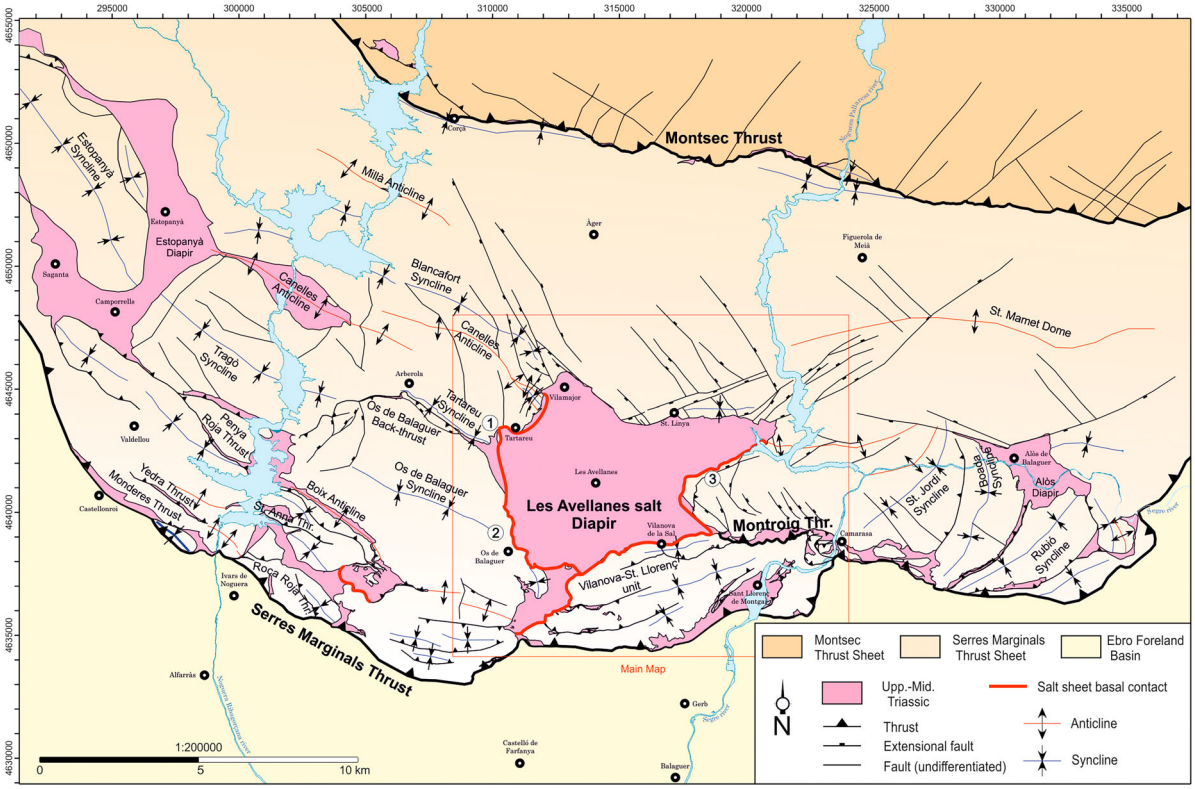

Figure 3. Structural map of the Les Avellanes Diapir area and surroundings with Triassic exposures. 1. Tartareu sub-basin, 2. Os de Balaguer sub-basin, and 3. Montroig sub-basin. See also the location of the Main Map (red square).

that folds grew during the early Eocene. Some anticlines, such as the Canelles Anticline, are box-shaped with wide hinges and Triassic rocks cropping out in the eroded cores (Figure 3, Main Map). Furthermore, the Canelles Anticline is intersected by oblique extensional faults similar to those at the northern diapir boundary. These faults displace stepping blocks downwards at the diapir contact (between Tartareu and Vilamajor villages, Main Map).

The eastern to south-eastern boundary of the Les Avellanes Diapir is dominated by the Montroig Thrust, which has a W-E strike and continuously outcrops eastwards up to the Segre River (Figure 3). This thrust was emplaced out of sequence, after the formation of the Serres Marginals Thrust (Teixell & Muñoz, 2000). The hangingwall of the Montroig Thrust, with upper Triassic rocks at its base, exposes a complete Jurassic sequence up to 800 m thick unconformably overlaid by the Upper Cretaceous units. Both of these units are truncated by NW-SE extensional faults, mainly dipping towards the NE. The footwall of the Montroig Thrust corresponds to the eastern termination of the Vilanova-Sant Llorenç unit, which is a detached tectonic unit emplaced over the Ebro Foreland Basin. This unit is characterized by a late Eocene to early Oligocene thin and incomplete stratigraphic sequence relative to the northern Serres Marginals cover, deformed by an imbricated system of short-wavelength folds and thrusts (Main Map). The thin stratigraphy in this unit is related to a condensed deposition and the presence of internal unconformities found at the southern termination of the Pyrenean Basin.

4.2. Stratigraphical, sedimentological, and petrological constraints on diapir emplacement

The Tartareu, Os de Balaguer, and Montroig sub-basins show a similar late Eocene to Oligocene sedimentary record that constrains the salt sheet emplacement. These sub-basins are adjacent to the diapir body and occupy structural lows formed by folding or faulting. Each section can be divided into two main intervals separated by erosional unconformities (Figure 4):

The lower interval is characterized by evaporitic facies that are stratigraphically enclosed by late Eocene-early Oligocene alluvial conglomerates. Evaporitic units (Figure 5A) lay on top of conglomerates at the core of the Os de Balaguer and the Tartareu sub-basins, and in the Montroig Thrust footwall. These units overlap the previous stratigraphy postdating tectonic deformation (Main Map) (Figure 4, sections 3 and 4). The enclosing alluvial conglomerates rapidly evolve laterally from massive, proximal facies to distal facies, where they are intercalated with fine-bedded sandstones and mudrocks (Figure 4, sections 1, 2, and 5 and Figure 5B). Clast composition, mainly limestones from the Jurassic, Upper Cretaceous, Paleocene, and lower Eocene units, indicates that

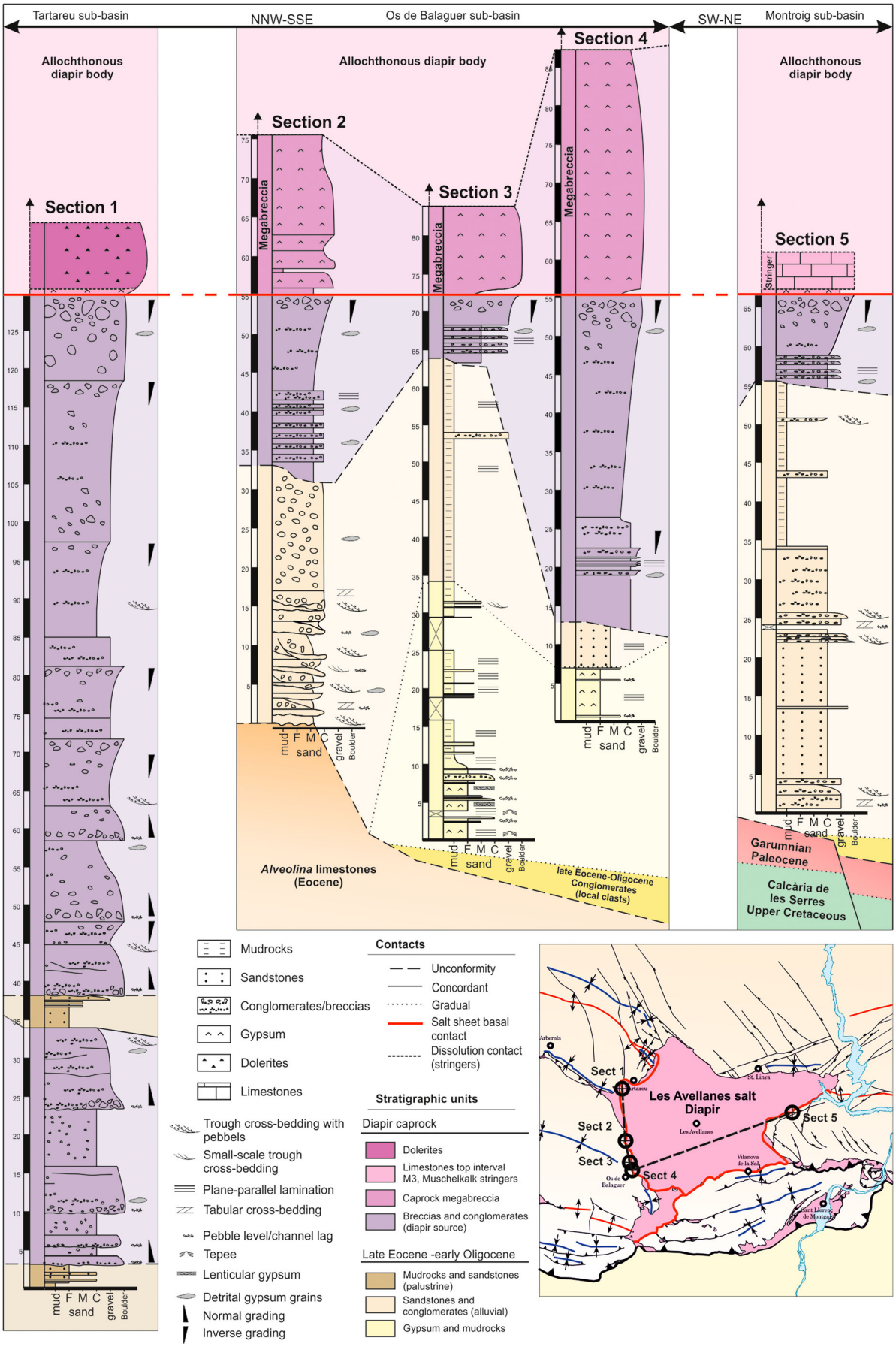

Figure 4. Stratigraphical sections and correlation (see their location in the map at the right bottom corner of the figure. Sub-basins locations are in Figure 3 and in the Main Map). In all studied locations the salt sheet extrusion covers a conglomeratic/breccia deposit (debrites) derived from the erosion of the diapir and emplaced under it. This supports the extension and emplacement of the diapir body as a salt sheet that advanced southwards, originated along the northern boundary where the salt migrated towards the surface.

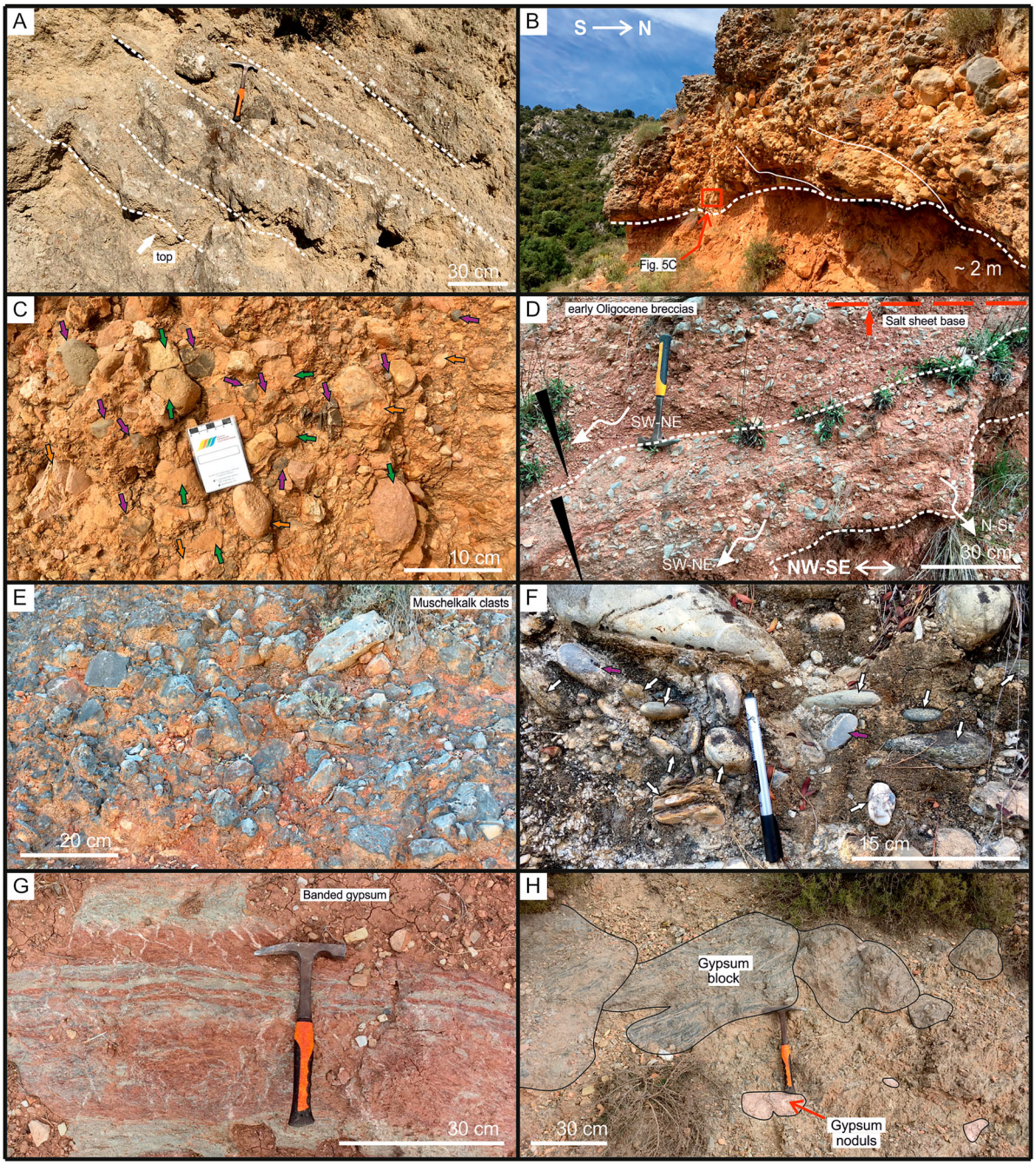

Figure 5. (A). Tabular gypsum beds at the Tartareu sub-basin with minor intercalation of mudrocks. Gypsum nodules are also observed. White arrow shows stratigraphic polarity. (B) Oligocene conglomerates at the southern diapir boundary (Os de Balaguer sub-basin). The deposit is organized in channel-like bodies with cross-bedding at the base interbedded with red mudrocks (see also Figure 4). (C). Close view from the facies described in Figure 5B. These conglomerates present a polymictic composition mainly derived from the erosion of the Serres Marginals units, contrasting with the northern conglomeratic facies. Pink arrows point towards Muschelkalk clasts, green arrows to Calcàrea de les Serres clasts, and orange arrows to *Alveolina* Limestones clasts (see Figure 5F). (D) Depositional breccias and conglomerates (debrites) exposed along the Montroig sub-basin (See also Figure 4). The deposit is typically organized in inverse graded beds with erosional bases. Paleocurrent senses in addition of compositions support that these breccias resulted from the erosion, mass-transport, and sedimentation of the diapir body rocks (Ghassemi & Roustaei, 2021). This deposit is overridden by the salt and thus lies beneath the diapir body (megabreccia) in all the studied sections (Figure 4). (E) Close-up view of the facies described in Figure 5D. These breccias are monomictic, composed of fragments derived from the Muschelkalk carbonate stringers, and clast-supported. (F) Oligocene conglomerates at the northern diapir boundary, postdating the Les Avellanes lateral extrusion. There is a prevalence of metamorphic and igneous rock fragments derived from the Pyrenean Axial Zone. (G) Banded gypsum facies located along the northern diapir exposure. (H) Megabreccia facies. Blocks of deformed, laminated gypsum floating in a fine matrix with gypsum nodules. This matrix contains a high percentage of mudrocks and carbonate milimeter-sized inclusions which gives a 'dirty' aspect.

conglomerates were formed by the erosion of the Serres Marginals reliefs without any major contribution from the Pyrenean hinterland. Triassic clasts are also present, indicating the erosion of the diapir, which was exposed during the progressive filling of these sub-basins (Figure 5C).

The upper interval is characterized by breccias and conglomerates sourced exclusively from the erosion of the diapir units, since they are made of gypsum, Muschelkalk carbonates, and dolerite clasts (Figure 5D and E). The internal architecture of this interval shows an upwards transition from normal-graded to inverse-graded beds, with a level of significantly bigger blocks, up to 60 cm in diameter, of dolerites and Muschelkalk carbonates with gypsum clasts, accumulated atop. The base of this interval is an unconformity caused by the erosion of the previous sequence, except in the Tartareu sub-basin (Figure 4, section 1) where these breccias are interbedded with the sub-basin infill (lower interval). In all studied locations this upper breccia interval is directly overlain by the diapir body (Figure 4).

Along the northwestern and northeastern diapir boundaries, Oligocene conglomerates and sandstones overlap the diapir body and preserve the extensional faults that bound the northern contact (in Vilamajor village and close to the Pantà de Camarasa, Main Map). A similar relationship is observed in a section of the southern boundary, between Os de Balaguer and Vilanova de la Sal villages. However, these three locations are the only ones where this relationship occurs, as generally the diapir is emplaced on top of the clastic facies. On the other hand, clast composition is well-differentiated in northern and southern areas, since the northern conglomerates contain abundant fragments of metamorphic and plutonic rocks transported from the Axial Zone (Figure 5F).

4.3. The Les Avellanes Diapir body

The Les Avellanes Diapir displays an apparent chaotic arrangement of mappable, decameter-thick carbonate M3 (Muschelkalk) stringers and dolerite bodies embedded within Keuper gypsum and mudrocks.

The Muschelkalk stringers are formed of two clearly different stratigraphic intervals: (1) a basal alternation of laminated limestones and marls overlaid by, (2) well-bedded, tabular limestones with minor intercalated thin levels of marls, which allow to establish the stratigraphic polarity of these stringers. Across the diapir exposure, the presence and disposition of the M3 stringers vary from north to south (Main map). In the northern region, the abundance of stringers is lower in comparison to the central and southern parts where they are relatively accumulated. In the northern area, they are located towards the NW, between Tartareu and Vilamajor villages, and the NE, close to Santa Linya (Main Map), where they are vertically emplaced, subparallel to the diapir contact. Conversely, in the central part where they are concentrated, around the Les Avellanes village (Main Map), they are horizontally stacked or overturned. Along the southern boundary, they are imbricated and primarily show a southwards vergence.

Likewise, the caprock matrix embedding the stringers also exhibits different facies from north to south. In the north, the caprock matrix facies are predominantly composed of banded gypsum with minor content of mudrocks and carbonates (Figure 5G). However, towards the south, along with the increasing number of outcropping M3 stringers, the gypsum is significantly more altered and mixed with accumulations of mudrocks and carbonates. These caprock matrix facies present deformation bands with mylonitic fabrics (named foliated gypsum, Main Map) suggesting the combination of brittle and ductile deformation related to the diapir evolution. In addition, in the Os de Balaguer sub-basin and in the Montroig sub-basin, the base of the diapir body is characterized by a megabreccia featuring meter to decameter blocks of gypsum and Muschelkalk stringers surrounded by a fine matrix, partially cemented with sulphates (Figure 5H). This megabreccia is emplaced over the late Eocene-early Oligocene sedimentary units (Figure 4) and shows a characteristic sequence where ductile shear deformation (foliations and lineations) is preferentially concentrated along its base. The megabreccia was interpreted as a dissolution breccia, or a debrite-like deposit created by the disaggregation of the caprock at the frontal lobe of the salt sheet and subsequently overrode by the spreading salt (Cofrade et al., 2023). The deformation was probably produced during the forward advance of the salt sheet as an intrasalt basal shear-band (Cofrade et al., 2023).

5. Discussion

The structural relationships between the diapir and the main tectonic elements in the area, as well as the stratigraphical, sedimentological, and petrological observations, allow us to differentiate between the two parts that form the Les Avellanes Diapir geometry, the extrusive salt sheet and the columnar feeder diapir, as well as the timing of its emplacement (Main Map).

5.1. The Les Avellanes Diapir geometry

The extensional faults, oblique to the contractive structures (Figure 3), form the northern boundary of the diapir. Late Eocene-Oligocene sediments fill the associated grabens and ultimately postdate the extensional deformation, which is dated to the late Eocene-Oligocene. These faults are associated with the collapse of the overburden caused by the migration of the salt towards the diapir stem, and therefore also constrain diapirism to the late Eocene-Oligocene. Thus, the northern part of the diapir exposure is interpreted as the Les Avellanes Diapir feeder. The mobilization of the salt in the study

area was probably triggered by the onset of synorogenic deformation, which started along the Serres Marginals during early Ypresian times (Muñoz, 1992; Muñoz, 2017), and is recorded by the existence of growth strata architectures in the *Alveolina* Limestones. The subsequent erosion of the elevated salt-cored contractive structures exposed the salt, initiating diapirism. This is constrained by the regional erosive surface at the base of the late Eocene-Oligocene series, that records the incision of the drainage network during the onset of orogenic deformation in the Serres Marginals.

The late Eocene-early Oligocene facies below the megabreccia in the Os de Balaguer sub-basin (Figure 4, sections 2, 3 and 4) are interpreted as the sedimentological record of the advance of an extrusive salt sheet laterally spreading by gravity from the feeder (Cofrade et al., 2023). The same facies, overlain by the megabreccia, are recorded in the Tartareu and Montroig sub-basins (Figure 4), and therefore, the salt sheet basal contact can be interpreted by the stratigraphic correlation of these facies along the diapir boundary. The trace and location of this contact suggest that a salt sheet advanced southward covering younger stratigraphy, although the precise extension of the coverage is not recorded.

The two parts of the Les Avellanes Diapir geometry, the diapir feeder in the north and the salt sheet in the south, are also supported by the structural configuration of the M3 stringers and the composition of the diapir body since the internal architecture of a salt structure reflects its evolution (Jackson & Hudec, 2017; Talbot & Aftabi, 2004; Talbot & Jackson, 1987). On the one hand, the arrangement formed by the stringers within the diapir body is the product of different salt flow kinematics during different stages of diapirism and can be preserved in the dissolution residue of an extruding diapir (Alsop et al., 2015; Amri et al., 2020; Jackson & Hudec, 2017; Talbot & Jackson, 1987). The stringers in the Les Avellanes diapir are subvertical along the northern contact and horizontally stacked in the central and southern areas. Therefore, their configuration reflects the vertical flow that characterizes a diapir stem (Sarkarinejad et al., 2018) and the subhorizontal flow during the advance of the salt sheet, respectively (Ghassemi & Roustaei, 2021; Jackson & Hudec, 2017). On the other hand, the residue left after the salt dissolution that surrounds the stringers (Cofrade et al., 2023) is made of gypsum with different proportions of embedded mudrocks and other insoluble components, and gradually transforms from north to south. In the northern area, where the feeder is inferred to be, the dominant lithology is gypsum (gypsum caprock, Main Map). However, towards the south, the content of mudrocks and carbonate within the gypsum (mixed caprock, Main Map) increases. The increasing percentage of mudrocks in the caprock matrix is in agreement with a higher degree of alteration, which is usually present at the frontal part of an extrusive salt sheet versus its feeding area, as the salt sheet further transforms during its advance (Nekouei & Zarei, 2016; Závada et al., 2021). Nevertheless, the gradual increase in mudrocks and carbonates towards the salt sheet frontal area may reflect lithological variations in the depositional Middle to Upper Triassic salt sequence. Diapirs show a concentrical internal zonation inherited from the stratigraphical architecture of the salt source sequence where lower, older units are in the core of the structure surrounded by younger, upper units. As salt extrudes laterally to form a salt sheet/namakier (Ghassemi & Roustaei, 2021)., this zonation rotates, so the older units occupy the core of the allochthonous sheet and the younger upper units tend to be located along its front (Dooley et al., 2015; Talbot & Aftabi, 2004; Talbot & Pohjola, 2009). Therefore, since the upper Keuper interval (K2-K3) contains more mudrocks interbeds, an enrichment of this lithology within the caprock matrix is expected along the frontal part of the salt sheet. Thus, given the sedimentological and stratigraphical relations observed along the southern boundary of the Les Avellanes Diapir, as well as the internal architecture of the diapir body, the southern part of the diapir exposure is interpreted as an extrusive salt sheet/namakier that extruded from a feeder diapir.

5.2. Relative timing of the salt sheet emplacement

The sedimentological and stratigraphical relationships between the salt extrusion and the deposition of the Oligocene conglomerates constrain the timing for the emplacement of the salt sheet. The different clast composition observed in the Oligocene conglomerates north and south of the diapir is explained by the existence of a barrier formed by the dynamic bulge over the feeder, deflecting the southwards arrival of sediments sourced in the Axial Zone. The isolation of the sub-basins from the regional depositional pathways (NE to SW, Garcés et al., 2020), reduced the sedimentation rate in the southern sub-basins during the salt extrusion, so the salt sheet advance was registered in these areas. Oligocene conglomerates postdate the feeder (NW and NE areas) and part of the southern boundary (east of the Os de Balaguer village). These conglomerates also postdate the Pyrenean structures and thus, the salt sheet extrusion is dated to the late Eocene-early Oligocene.

6. Concluding remarks

Mapped structural features, together with the stratigraphical, sedimentological, and petrological

correlations support the hypothesis that the Les Avellanes Diapir geometry resulted from the combination of two different salt structures, an extrusive salt sheet, and a feeder diapir located along the northern diapir exposure from where the salt spread laterally and advanced southwards, covering the southern low areas.

The Triassic salt migrated and accumulated in the Serres Marginals during the Eocene-Oligocene due to the Pyrenean deformation. The detached anticline hinges collapsed, as recorded in the system of conjugate extensional faults oblique to the contractive structures, facilitating the expulsion of the Triassic salt towards the surface in the northern area, thus interpreted as the feeder. A salt sheet emplacement is supported by the sedimentological and stratigraphical interpretation of the facies overlaid by the diapir body, as well as the internal architecture of the diapir body, so the salt sheet basal contact has been traced accordingly in the Main Map. Its emplacement occurred relatively fast during the late Eocene-early Oligocene and was later postdated by the Oligocene sedimentation.

Software

FieldMove® (Petroleum Experts) application was used for field-collected data and sketching, running in a high-performance tablet device with a GPS system integrated with a typical resolution of +- 2 m. Orthoimages (PNOA-IGN Plan Nacional de Ortofotografía Aérea – Instituto Geográfico Nacional, http://ign.es and ICGC 25 cm/px resolution, https://www.icgc.cat), DEM (LiDAR-based, 2 × 2 m resolution, IGCG, https://www.icgc.cat), and geological and topographic maps were projected in the same device and used during fieldwork (MAGNA 1:50000, http://info.igme.es; and IGCG 1:25000 series, https://www.icgc.cat). Data were then plotted and transformed into georeferenced vector files using the 3D software MOVE® (Petroleum Experts), then imported into ArcGIS Pro software where the Main Map was constructed, also importing the mentioned cartographic database to fine-tuning the geological contacts and to improve accuracy. Symbology was designed according to a standard geological library and adapted when necessary.

Acknowledgments

Josep Anton Muñoz, Daniel Muñoz-López, Oriol Vilanova, Hanneke Heida, and Yetong Wang are gratefully acknowledged for their fieldwork assistance. We also thank Dr Vít Pászto, Dr Prokop Závada, and Dr Mohammad R. Ghassemi for their very constructive reviews.

Victoriano Pineda, who also helped greatly during fieldwork and discussions, is especially acknowledged. Your friends and collages will always remember you.

Disclosure statement

No potential conflict of interest was reported by the author(s).

Funding

This research was performed within the framework of the research project SABREM (PID2020-117598GB-C21), SALTCONBELT (CGL2017-85532-P), and DGICYT (PID2021-122467NB-C22) funded by Ministerio de Ciencia, Innovación y Universidades/Agencia Estatal de Investigación/Fondo Europeo de Desarrollo Regional, Unión Europea, and the Grup de Recerca Reconegut per la Generalitat de Catalunya 2021 SGR-Cat 00349 'Geologia Sedimentària' and 2021SGR76 'Geodinàmica i Anàlisi de Conques'. GC also acknowledges the support of the UB scholarship PREDOC-UB19/20 5660400.

Data availability statement

The authors confirm that the data supporting the findings of this study are available within the article and its supplementary materials.

References

Institut Cartogràfic de Catalunya, Mapa geològic de Catalunya, [Àger 327-2-1 (64-25)]. 1:25.000 (1a edició), Cartografia geològica GT I, Barcelona (2008), ISBN 841-47-745-0044-4

Institut Cartogràfic de Catalunya, Mapa geològic de Catalunya, [Camarasa 328-1-2 (65-26)]. 1:25.000 (1a edició), Cartografia geològica GT I, Barcelona (2014), ISBN 978-84-393-9128-9

Institut Cartogràfic de Catalunya, Mapa geològic de Catalunya, [Figuerola de Meià 328-1-1 (65-25)]. 1:25.000 (1a edició), Cartografia geològica GT I, Barcelona (2007), ISBN 841-47-745-0039-0

Institut Cartogràfic de Catalunya, Mapa geològic de Catalunya, [Os de Balaguer 327–2-2 (64–26)]. 1:25.000 (1a edició), Cartografia geològica GT I, Barcelona (2010), ISBN 841-47-745-0054-3.

Alsop, G. I., Weinberger, R., Levi, T., & Marco, S. (2015). Deformation within an exposed salt wall: Recumbent folding and extrusion of evaporites in the Dead Sea Basin. *Journal of Structural Geology*, *70*, 95–118. https://doi.org/10.1016/j.jsg.2014.11.006

Amri, Z., Naji, C., Masrouhi, A., & Bellier, O. (2020). Interconnection Salt Diapir–allochthonous salt sheet in northern Tunisia: The Lansarine–Baoula case study. *Journal of African Earth Sciences*, *170*, 103876, 1-16. https://doi.org/10.1016/j.jafrearsci.2020.103876

Angrand, P., & Mouthereau, F. (2021). Evolution of the Alpine orogenic belts in the western Mediterranean region as resolved by the kinematics of the Europe-Africa diffuse plate boundary. *BSGF - Earth Sciences Bulletin*, *192*, 42. https://doi.org/10.1051/bsgf/2021031

Ayala, C., Rey-Moral, C., Rubio, F., Soto, R., Clariana, P., Martín-León, J., Bellmunt, F., Gabàs, A., Macau, A., Casas, A. M., Martí, J., Pueyo, E. L., & Benjumea, B. (2021). Gravity data on the Central Pyrenees: A step forward to help a better understanding of the Pyrenean structures. *Journal of Maps*, *17*(2), 750–759. https://doi.org/10.1080/17445647.2021.2001386

Beaumont, C., Muñoz, J. A., Hamilton, J., & Fullsack, P. (2000). Factors controlling the Alpine evolution of the Central Pyrenees inferred from a comparison of observations and geodynamical models. *Journal of Geophysical Research: Solid Earth*, *105*(B4), 8121–8145.

Borradaile, G. J. (2015). *Understanding geology through maps*. Elsevier. ISBN: 9780128008669. https://doi.org/10.1016/c2013-0-18872-1.

Burrel, L., & Teixell, A. (2021). Contractional salt tectonics and role of pre-existing diapiric structures in the South Pyrenean foreland fold-and-thrust belt (Montsec and Serres Marginals). *Journal of the Geological Society*, *178*. https://doi.org/10.1144/jgs2020-085

Callot, J.-P., Salel, J.-F., Letouzey, J., Daniel, J.-M., & Ringenbach, J.-C. (2016). Three-dimensional evolution of salt-controlled minibasins: Interactions, folding and megaflap development. *AAPG Bulletin*, *100*(09), 1419–1442. https://doi.org/10.1306/03101614087

Calvet, F., Anglada, E., & Salvany, J. M. (2004). El Triásico de los Pirineos. In J. A. Vera (Ed.), *Geología de España* (pp. 272–274). Sociedad Geológica de España and Instituto Geológico y Minero de España.

Calvet, M., Gunnell, Y., & Laumonier, B. (2021). Denudation history and paleogeography of the Pyrenees and their peripheral basins: An 84-million-year geomorphological perspective. *Earth-Science Reviews*, *215*, 103436. https://doi.org/10.1016/j.earscirev.2020.103436

Camara, P., & Flinch, J. (2017). The Southern Pyrenees: A salt-based fold and thrust belt. In J. I. Soto, J. F. Flinch, & G. Tari (Eds.), *Permo-Triassic Salt Provinces of Europe, North Africa and the Atlantic Margins. Elsevier. Tectonics and hydrocarbon potential* (pp. 395–415). Elsevier.

Casini, G., Vergés, J., Drzewiecki, P., Ford, M., Cruset, D., Wright, W., & Hunt, D. (2023). Reconstructing the Iberian salt-bearing rifted margin of the Southern Pyrenees: Insights from the Organyà Basin. *Tectonics*, *42*(7), https://doi.org/10.1029/2022tc007715

Cofrade, G., Cantarero, I., Gratacós, Ò, Ferrer, O., Ramirez-Perez, P., Travé, A., & Roca, E. (2023). Allochthonous salt advance recorded by the adjacent syn-kinematic sedimentation: Example from the les Avellanes diapir (South Central Pyrenees). *Global and Planetary Change*, *220*, 1–26, 104020. https://doi.org/10.1016/j.gloplacha.2022.104020

Cruset, D., Vergés, J., Albert, R., Gerdes, A., Benedicto, A., Cantarero, I., & Travé, A. (2020). Quantifying deformation processes in the SE Pyrenees using U–Pb dating of fracture-filling calcites. *Journal of the Geological Society*, *177*(6), 1186–1196. https://doi.org/10.1144/jgs2020-014

Dooley, T. P., Jackson, M. P., & Hudec, M. R. (2015). Breakout of squeezed stocks: Dispersal of roof fragments, source of extrusive salt and interaction with regional thrust faults. *Basin Research*, *27*(1), 3–25. https://doi.org/10.1111/bre.12056

Duffy, O., Dooley, T., Hudec, M., Jackson, M., Fernandez, N., Jackson, C., & Soto, J. (2018). Structural evolution of salt-influenced fold-and-thrust belts: A synthesis and new insights from basins containing isolated salt diapirs. https://doi.org/10.31223/osf.io/nd7et

Espurt, N., Angrand, P., Teixell, A., Labaume, P., Ford, M., de Saint Blanquat, M., & Chevrot, S. (2019). Crustal-scale balanced cross-section and restorations of the Central Pyrenean Belt (nestes-cinca transect): Highlighting the structural control of Variscan Belt and Permian-Mesozoic rift systems on Mountain Building. *Tectonophysics*, *764*, 25–45. https://doi.org/10.1016/j.tecto.2019.04.026

Fillon, C., Gautheron, C., & Van der Beek, P. (2013). Oligocene–miocene burial and exhumation of the Southern Pyrenean foreland quantified by low-temperature thermochronology. *Journal of the Geological Society*, *170*(1), 67–77. https://doi.org/10.6084/m9.figshare.3453161.v1

Garcés, M., López-Blanco, M., Valero, L., Beamud, E., Muñoz, J. A., Oliva-Urcia, B., Vinyoles, A., Arbués, P., Cabello, P., & Cabrera, L. (2020). Paleogeographic and sedimentary evolution of the south Pyrenean foreland basin. *Marine and Petroleum Geology*, *113*, 104105. https://doi.org/10.1016/j.marpetgeo.2019.104105

García-Senz, J. (2002). *Cuencas extensivas del Cretácico Inferior en los Pirineos Centrales. Formación y subsecuente inversión. Tesis doctoral*. Universitat de Barcelona.

Ghassemi, M. R., & Roustaei, M. (2021). Salt extrusion kinematics: Insights from existing data, morphology and InSAR modelling of the active emergent Anguru diapir in the Zagros fold and thrust belt, Iran. *Journal of the Geological Society*, *178*(6), 15. https://doi.org/10.1144/jgs2020-136

Gómez-Gras, D., Roigé, M., Fondevilla, V., Oms, O., Boya, S., & Remacha, E. (2016). Provenance constraints on the Tremp Formation paleogeography (Southern Pyrenees): Ebro massif vs Pyrenees sources. *Cretaceous Research*, *57*, 414–427. https://doi.org/10.1016/j.cretres.2015.09.010

González-Esvertit, E., Canals, À, Bons, P. D., Murta, H., Casas, J. M., & Gomez-Rivas, E. (2022). Geology of giant quartz veins and their host rocks from the Eastern Pyrenees (Southwest Europe). *Journal of Maps*, *19*, 1–13. https://doi.org/10.1080/17445647.2022.2133642

Handy, M. R., Schmid, S. M., Bousquet, R., Kissling, E., & Bernoulli, D. (2010). Reconciling plate-tectonic reconstructions of Alpine Tethys with the geological-geophysical record of spreading and subduction in the Alps. *Earth-Science Reviews*, *102*(3–4), 121–158. https://doi.org/10.1016/j.earscirev.2010.06.002

Jackson, M., & Hudec, M. (2017). Internal deformation in salt bodies. In *Salt tectonics: Principles and practice* (pp. 181–228). Cambridge University Press. https://doi.org/10.1017/9781139003988.011.

Jurado, M. J. (1990). El triásico y el liásico basal evaporíticos del subsuelo de la cuenca del Ebro. In F. Ortí, & J. M. Salvany (Eds.), *Formaciones evaporíticas de la Cuenca del Ebro y cadenas periféricas, y de la zona de Levante* (pp. 21–28). Nuevas aportaciones y guía de superficie.

Klimowitz, J., & Torrescusa, S. (1990). Notas sobre la estratigrafia y facies de la serie triásica en el Alóctono Surpirenico. In F. Orti & J. M. Salvany (Eds.), *Formaciones evaporíticas de la Cuenca del Ebro y cadenas periféricas, y de la zona de Levante. Nuevas aportaciones y guía de superficie* (pp. 29–33). ENRESA and GPPG, Barcelona.

Lanaja, J. M. (1987). Contribución de la exploración petrolífera al conocimiento de la geología de España. (edt.) IGME and Universidad Politécnica de Madrid. ISBN 8474743982.

López-Gómez, J., et al. (2019). Permian-triassic rifting stage. In C. Quesada & J. Oliveira (Eds.), *The geology of iberia: A geodynamic approach. Regional geology reviews*. Springer. https://doi.org/10.1007/978-3-030-11295-0_3

Lopez-Mir, B., Muñoz, J. A., & García-Senz, J. (2015). Extensional salt tectonics in the partially inverted Cotiella post-rift basin (south-central Pyrenees):

Structure and evolution. *International Journal of Earth Sciences*, *104*(2), 419–434. https://doi.org/10.1007/s00531-014-1091-9

Lopez-Mir, B., Muñoz, J. A., & García-Senz, J. (2016). Geology of the cotiella thrust sheet, Southern Pyrenees (Spain). *Journal of Maps*, *12*(sup1), 323–327. https://doi.org/10.1080/17445647.2016.1211895

Martinez-Peña, M., & Casas-Sainz, A. (2003). Cretaceous–tertiary tectonic inversion of the Cotiella Basin (southern Pyrenees, Spain). *International Journal of Earth Sciences*, *92*(1), 99–113. https://doi.org/10.1007/s00531-002-0283-x

Martín-Martín, J. D., Vergés, J., Saura, E., Moragas, M., Messager, G., Baqués, V., Razin, P., Grélaud, C., Malaval, M., Joussiaume, R., Casciello, E., Cruz-Orosa, I., & Hunt, D. W. (2017). Diapiric growth within an early jurassic rift basin: The tazoult salt wall (central high atlas, Morocco). *Tectonics*, *36*(1), 2–32. https://doi.org/10.1002/2016tc004300

McClay, K., Muñoz, J. A., & García-Senz, J. (2004). Extensional salt tectonics in a contractional orogen: A newly identified tectonic event in the Spanish Pyrenees. *Geology*, *32*(9), 737–740. https://doi.org/10.1130/G20565.1

Muñoz, J. A. (1992). Evolution of a continental collision belt: ECORS-pyrenees crustal balanced cross-section. *Thrust Tectonics*, 235–246. https://doi.org/10.1007/978-94-011-3066-0_21

Muñoz, J. A. (2002). The Pyrenees. In W. Gibbons & T. Moreno (Eds.), *The geology of Spain. The geological society of London* (pp. 370–385). https://doi.org/10.1144/GOSPP

Muñoz, J. A. (2017). Fault-related folds in the Southern Pyrenees. *AAPG Bulletin*, *101*(04), 579–587. https://doi.org/10.1306/011817DIG17037

Muñoz, J.-A., Beamud, E., Fernández, O., Arbués, P., Dinarès-Turell, J., & Poblet, J. (2013). The Ainsa Fold and thrust oblique zone of the central Pyrenees: Kinematics of a curved contractional system from paleomagnetic and structural data. *Tectonics*, *32*(5), 1142–1175. https://doi.org/10.1002/tect.20070

Muñoz, J. A., Mencos, J., Roca, E., Carrera, N., Gratacós, O., Ferrer, O., & Fernández, O. (2018). The structure of the South-Central-Pyrenean fold and thrust belt as constrained by subsurface data. *Geol. Acta*, *16*(4), 439–460. https://doi.org/10.1344/GeologicaActa2018.16.4.7

Muñoz-López, D., Cruset, D., Vergés, J., Cantarero, I., Benedicto, A., Mangenot, X., Albert, R., Gerdes, A., Beranoaguirre, A., & Travé, A. (2022). Spatio-temporal variation of fluid flow behavior along a fold: The bóixols-sant corneli anticline (southern Pyrenees) from U–pb dating and structural, petrographic and geochemical constraints. *Marine and Petroleum Geology*, *143*, 105788. https://doi.org/10.1016/j.marpetgeo.2022.105788

Nekouei, E., & Zarei, M. (2016). Karst hydrogeology of Karmustadj salt diapir, southern Iran. *Carbonates and Evaporites*, *32*(3), 315–323. https://doi.org/10.1007/s13146-016-0298-1

Odlum, M. L., Stockli, D. F., Capaldi, T. N., Thomson, K. D., Clark, J., Puigdefàbregas, C., & Fildani, A. (2019). Tectonic and sediment provenance evolution of the South Eastern Pyrenean foreland basins during rift margin inversion and orogenic uplift. *Tectonophysics*, *765*, 226–248. https://doi.org/10.1016/j.tecto.2019.05.008

Olivet, J. L. (1996). La cinématique de la plaque ibérique. *Bulletin des Centres de Recherches Exploration-Production Elf-Aquitaine*, *20*(1), 131–195.

Ortí, F. (1987). Aspectos sedimentológicos de las evaporitas del Triásico y del Liásico inferior en el E de la Península Ibérica. *Cuadernos de Geología Ibérica*, *11*, 837–858.

Ortí, F., García-Veigas, J., Rosell, L., Jurado, M. J., & Utrilla, R. (1996). Formaciones salinas de las cuencas triásicas en la Península Ibérica: caracterización petrológica y geoquímica. *Cuadernos de Geología Ibérica*, *20*, 13–35.

Ortí, F., Pérez-López, A., & Salvany, J. M. (2017). Triassic evaporites of Iberia: Sedimentological and palaeogeographical implications for the western neotethys evolution during the Middle Triassic–earliest jurassic. *Palaeogeography, Palaeoclimatology, Palaeoecology*, *471*, 157–180. https://doi.org/10.1016/j.palaeo.2017.01.025

Pocoví, A. (1978). Estudio geológico de las Sierras Marginales Catalanas (Prepirineo de Lérida) Tesis Doctoral, Univ, de Barcelona (1978).

Pujalte, V., Baceta, J., Schmitz, B., Orue-Echebarría, X., Payros, A., Bernaola, G., Apellaniz, E., Caballero, F., Robador, A., Serra-Kiel, J., & Tosquella, J. (2009). Redefinition of the Ilerdian Stage (early Eocene). *Geol. Acta*, *7*(1–2), 177–194.

Ramirez-Perez, P., Cantarero, I., Cofrade, G., Muñoz-López, D., Cruset, D., Sizun, J.-P., & Travé, A. (2023). Petrological, petrophysical and Petrothermal Study of a folded sedimentary succession: The Oliana Anticline (Southern Pyrenees), outcrop analogue of a geothermal reservoir. *Global and Planetary Change*, *222*, 104057. https://doi.org/10.1016/j.gloplacha.2023.104057

Ramos, A., Lopez-Mir, B., Wilson, P. E., Granado, P., & Muñoz, J. A. (2020). 3D reconstruction of syn-tectonic strata in a salt-related orogen: Learnings from the Llert Syncline (south-central Pyrenees). *Geologica Acta*, *18*, 1–19. https://doi.org/10.1344/geologicaacta2020.18.20

Roca, E., Ferrer, O., Rowan, M. G., Muñoz, J. A., Butillé, M., Giles, K. A., Arbués, P., & de Matteis, M. (2021). Salt tectonics and controls on halokinetic-sequence development of an exposed deepwater diapir: The Bakio Diapir, Basque-cantabrian basin, Pyrenees. *Marine and Petroleum Geology*, *123*, 104770. https://doi.org/10.1016/j.marpetgeo.2020.104770

Rowan, M. G., Hearon IV, T. E., Kernen, R. A., Giles, K. A., Gannaway-Dalton, C. E., Williams, N. J., Fiduk, J. C., Lawton, T. F., Hannah, P. T., & Fischer, M. P. (2019). A review of allochthonous salt tectonics in the Flinders and Willouran Ranges, South Australia. *Australian Journal of Earth Sciences*, *67*(6), 787–813. https://doi.org/10.1080/08120099.2018.1553063

Salvany, J. M. (1999). Diapirismo triásico antiguo y reciente en el Anticlinal de Canelles, Sierras Marginales Catalanas (zona surpirenaica central). *Rev. Soc. Geol. España*, *12*(2), 149–164.

Salvany, J. M., & Bastida, J. C. (2004). Análisis litoestratigráfico del Keuper Surpirenaico Central. *Rev. Soc. Geol. España*, *17*(1–2), 3–26.

Santolaria, P., Casas-Sainz, A. M., Soto, R., Pinto, V., & Casas, A. (2014). The Naval diapir (southern Pyrenees): Geometry of a salt wall associated with thrusting at an oblique ramp. *Tectonophysics*, *637*, 30–44. https://doi.org/10.1016/j.tecto.2014.09.008

Santolaria, P., Granado, P., Wilson, E. P., de Matteis, M., Ferrer, O., Strauss, P., Pelz, K., König, M., Oteleanu, A. E., Roca, E., & Muñoz, J. A. (2022a). From salt-bearing rifted margins to fold-and-thrust belts. Insights from analog modeling and Northern Calcareous Alps Case Study. *Tectonics*, *41*(11), https://doi.org/10.1029/2022tc007503

Santolaria, P., Harris, L. B., Casas, A. M., & Soto, R. (2022b). Influence of décollement-cover thickness variations in fold-and-thrust belts: Insights from Centrifuge Analog

Modeling. *Journal of Structural Geology*, *163*, 104704. https://doi.org/10.1016/j.jsg.2022.104704

Sarkarinejad, K., Sarshar, M. A., & Adineh, S. (2018). Structural, micro-structural and kinematic analyses of channel flow in the Karmostaj salt diapir in the Zagros foreland folded belt, Fars province, Iran. *Journal of Structural Geology*, *107*, 109–131. http://doi.org/10.1016/j.jsg.2017.12.005

Saula, E., Samsó, J. M., Escuer, J., Casanovas, J., & Barnolas, A. (2000). Mapa geológico de España 1:50.000 (2ª serie), Hoja 328 (33-13), Artesa de Segre. Instituto Geológico y Minero de España, Madrid.

Saura, E., Ardèvol i Oró, L., Teixell, A., & Vergés, J. (2016). Rising and falling diapirs, shifting depocenters, and flap overturning in the Cretaceous Sopeira and Sant Gervàs Subbasins (Ribagorça Basin, southern Pyrenees). *Tectonics*, *35*(3), 638–662. https://doi.org/10.1002/2015tc004001

Séguret, M. (1972). Étude tectonique des nappes et séries décollées de la partie centrale du versant sud des Pyrénées – caractère synsédimentaire, rôle de la compression et de la gravité. Série Géologie Structurale, vol. 2, Publications de l'Universite des Sciences et Techniques du Languedoc (USTELA), Montpellier, France (1972), p. 155.

Sibuet, J. C., Srivastava, S. P., & Spakman, W. (2004). Pyrenean orogeny and plate kinematics. *J. Geophys. Res. Sol. Ea*, *109*(B8), 1–18. https://doi.org/10.1029/2003JB002514

Sussman, A. J., Butler, R. F., Dinarès-Turell, J., & Vergés, J. (2004). Vertical-axis rotation of a foreland fold and implications for orogenic curvature: An example from the Southern Pyrenees, Spain. *Earth and Planetary Science Letters*, *218*(3-4), 435–449. https://doi.org/10.1016/S0012-821X(03)00644-7

Talbot, C., & Aftabi, P. (2004). Geology and models of salt extrusion at Qum Kuh, central Iran. *Journal of the Geological Society*, *161*(2), 321–334. https://doi.org/10.1144/0016-764903-102

Talbot, C., & Jackson, M. (1987). Internal kinematics of salt diapirs. *AAPG Bulletin*, *71*(9), 1068–1093.

Talbot, C. J., & Pohjola, V. (2009). Subaerial salt extrusions in Iran as analogues of ice sheets, streams and glaciers. *Earth-Science Reviews*, *97*(1–4), 155–183. https://doi.org/10.1016/j.earscirev.2009.09.004

Teixell, A., & Barnolas, A. (1996). Mapa geológico de España 1:50.000 (2ª serie), Hoja 327 (32-13), Os de Balaguer. Instituto Geológico y Minero de España, Madrid.

Teixell, A., & Muñoz, J. A. (2000). Evolución tectono-sedimentaria del Pirineo meridional durante el Terciario: una síntesis basada en la transversal del río Noguera Ribagorçana. *Revista de la Sociedad Geológica de España*, *13*(2), 251–264.

Ullastre, J., & Masriera, A. (2004). Sobre la edad de los conglomerados basales de la transgresión del Senoniense en la parte más interna de la cuenca sudpirenaica catalana (NE de España). *Treballs del Museu de Geologia de Barcelona*, *2004*(12), 175–185. https://raco.cat/index.php/TreballsMGB/article/view/72455

Vergés, J., Fernàndez, M., & Martìnez, A. (2002). The pyrenean orogen: Pre-, syn-, and post-collisional evolution. *Journal of the Virtual Explorer*, *08*. https://doi.org/10.3809/jvirtex.2002.00058

Vergés, J., Millán, H., Roca, E., Muñoz, J. A., Marzo, M., Cirés, J., Bezemer, T. D., Zoetemeijer, R., & Cloetingh, S. (1995). Eastern Pyrenees and related foreland basins: Pre-, syn- and post-collisional crustal-scale cross-sections. *Marine and Petroleum Geology*, *12*(8), 903–915. https://doi.org/10.1016/0264-8172(95)98854-x

Vergés, J., & Muñoz, J. A. (1990). Thrust sequence in the southern Central Pyrenees. *Bulletin De La Société Géologique De France*, *VI*(2), 265–271. https://doi.org/10.2113/gssgfbull.vi.2.265

Vidal-Royo, O., Rowan, M. G., Ferrer, O., Fischer, M. P., Fiduk, J. C., Canova, D. P., Hearon, T. E., & Giles, K. A. (2021). The transition from Salt Diapir to weld and thrust: Examples from the northern Flinders Ranges in South Australia. *Basin Research*, *33*(5), 2675–2705. https://doi.org/10.1111/bre.12579

Závada, P., Bruthans, J., Adineh, S., Warsitzka, M., & Zare, M. (2021). Composition and deformation patterns of the caprock on salt extrusions in southern Iran – field study on the Karmostaj and Siah Taq Diapirs. *Journal of Structural Geology*, *151*, 104422. https://doi.org/10.1016/j.jsg.2021.104422